LiDAR Data Filtering Based on the Improved Window Size of Progressive Mathematical Morphology

Xianjian Lu[1,*], Le Luo[1], Bin Zhou[1], Yuhui Huang[1], Chenlong Wu[1]

1. College of Geomatics and Geoinformation, Guilin University of Technology, Guilin Guangxi 541004, China-2008056@glut.edu.cn

KEY WORDS: LiDAR; point cloud; morphology filtering; opening operation; window size; topographic features;

ABSTRACT:

Filtering is one of the core post-processing steps of airborne LiDAR point cloud data. It is difficult for traditional mathematical morphology filtering algorithms to preserve sudden terrain features, especially when using larger filtering windows. In this paper, an improved progressive mathematical morphology filtering algorithm is proposed to solve the problem which is difficult to filter out a large area of non-ground points effectively and causes omission filtering on prominent topographic features. First the elevation information of point cloud data is meshed, and then the opening operation (erosion and dilation) is performed. By improving the mathematical formula of window size, the window size and the corresponding elevation difference threshold are iterated continuously. Within each corresponding filtering window, objects that are larger than the size of the structural element window are retained, and objects smaller than the size of the structural element window are filtered. Fourteen samples provided by ISPRS committee were selected to test the performance of the proposed method. Experimental results show that the improved method can effectively filter out most of the non-ground points, and this method can achieve great results not only in urban flat areas, but also in the mountains. Compared with the traditional filtering methods, the filter performance of the new method proposed in this paper has been greatly improved. The method in this paper obtains the lower errors and retains the complex topographic features.

* Corresponding author

1. INTRODUCTION

LIDAR (Light Detection and Ranging) filtering is a challenging task, especially for area with high relief or hybrid geographic features (Wan et al., 2018). Over the past few years, many researchers have made a number of related researches. Reference (Kraus et al.,1998) utilized linear least squares interpolation iteratively to remove trees in urban areas. The iterative linear interpolation method removes a low-order polynomial trend surface from the original elevation data to generate a set of reduced elevation values. However, the iterative linear interpolation is not guaranteed to converge in urban areas where significant anthropogenic modification of natural terrain occurs. Reference (Vosselman, 2000) proposed a slope-based filter that identifies ground data by comparing slopes between a LIDAR point and its neighbors. However, the training datasets have to include all types of ground measurements in a study area to achieve good results. Both omission and commission errors were large when this method was applied to vegetated mountain areas with a considerable slope variation. Reference (Axelsson, 2000) suggested adaptive TIN models to find ground points in urban areas. The problem with the adaptive TIN method is that different thresholds are required to be given for various land cover types, and building TIN is a process that largely increases computation load for the magnitude of LIDAR data. Reference (Zhang et al., 2003) develops a progressive morphological filter. The laser points are firstly interpolated to generate a regular grid. Then morphological opening operation is performed iteratively to remove object points by gradually increasing the filter window size and the elevation difference thresholds. If the LIDAR data is of huge size, a very heavy workload of computation is a must.

Nevertheless, it is difficult to effectively filter non-ground points using the mathematical morphological filtering algorithm. By improving the size of the filtering window, an improved progressive mathematical morphology filtering algorithm is proposed to filter out larger area of object points and reduce the leakage phenomenon. The proposed algorithm is validated by the public test data published by ISPRS, and the effectiveness of the proposed improved method is verified, compared with the filtering performance of other algorithms.

2. MORPHOLOGY FILTERING

2.1 The Principle of Mathematical Morphological

Mathematical morphology composes operations based on set theory to extract features from an image (Haralick et al., 1987). The concept of erosion and dilation has been extended to gray scale images and corresponds to finding the minimum or maximum of the combinations of pixel values and the kernel function, respectively, within a specified neighborhood of each raster (Sun and Gu, 2016).

These concepts can also serve as extended to the analysis of a continuous surface such as a digital surface model as measured by LIDAR data (Li et al., 2013). If LiDAR points are considered as a regular gray scale grid image, then the shapes of buildings, cars, and trees can be identified by the change of gray. Therefore, erosion operation and dilation operation are defined as respectively in the grid DSM generated by the height information of LiDAR point cloud data:

$$Z_e(i,j) = (Z \otimes g)(i,j) = \min_{(s,t)\in\omega} [Z(s,t)], \quad (1)$$

$$Z_d(i,j) = (Z \oplus g)(i,j) = \max_{(s,t)\in\omega} [Z(s,t)], \quad (2)$$

where Z is grid DSM; g is structural element, $(Z \otimes g)$ is erosion operation, $(Z \oplus g)$ is dilation operation, $Z_e(i,j)$ and $Z_d(i,j)$ are grid elevation values with index (i,j) in DSM of grid after erosion operation and dilation operation, and ω is window size corresponding to structural elements. Combined erosion and dilation operation to form opening operation:

$$(Z \circ g)(i,j) = [(Z \otimes g) \oplus g](i,j), \quad (3)$$

For grid DSM, erosion operation is performed first, and then dilation operation is carried out. Objects larger than the window size of the structural elements can be retained while objects smaller than the window size of the structural elements can be removed. It has been extensively used in the field of LiDAR data filtering (Luo et al., 2009).

2.2 Progressive Mathematical Morphology

The selection of a filtering window size and the distribution of the building and trees in a specific area are critical for the success of this method. In an ideal situation, if a suitable window size is selected, all the object points can be separated by only one opening operation to obtain a digital elevation model (DEM). If a small window size is used in this method, only small objects (such as cars and trees) can be filtered (Kilian et al., 1996). The points corresponding to the tops of large-sized building complexes that often exist in urban areas cannot be filtered. On the other hand, the filter tends to over-remove the ground points with a large window size. However, it is quite difficult to filter with only a constant window size for different sizes of the various objects. Reference (Zhang et al., 2003) elaborated an incremental morphological filtering algorithm which was based on the idea of progressively increasing the size of the filtering window and the changing threshold of elevation difference. Compared with traditional mathematical morphology, this method can filter out various sizes of features. The data processing process is illustrated in Figure 1.

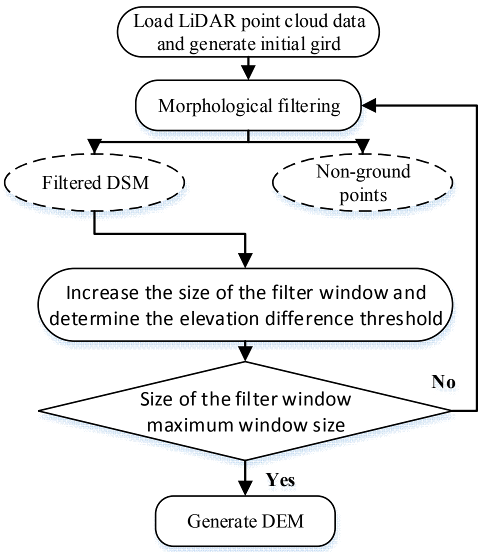

Figure 1. Flow chart filtering algorithm based on of the progressive multi-scale mathematical morphology

The size of the window is one of the most important steps in filtering non-ground points (Mongus and Žalik, 2012). The size of the window can be determined linearly or exponentially:

$$\omega_k = 2kb + 1 \tag{4}$$

where k = 1, 2, 3, ..., M; b is the initial window size.

$$\omega_k = 2b^k + 1 \tag{5}$$

where k = 1, 2, 3, ..., M; b is the cardinality of the exponential function.

To ensure that all ground objects are effectively filtered, the maximum area of the ground objects must be smaller than the window size of the last iteration. In order to retain the details of the geographic features in the filtering, s the elevation threshold of each iteration is set as:

$$dh_{T,K} = \begin{cases} dh_0, \omega_k \leq 3 \\ s \times (\omega_k - \omega_{k-1}) \times cellsize + dh_0, \omega_k > 3 \\ dh_{max}, dh_{T,K} > dh_{max} \end{cases} \tag{6}$$

where ω_k represents the window size of the kth filter; $cellsize$ is the grid spacing of the DSM; dh_0 and dh_{max} are the initial and maximum height difference thresholds respectively; s is the terrain slope parameter. It can be seen from the equation that as the filter window increases, the height difference threshold increases, and the magnitude of the increase is determined by the slope of the terrain. By judging that the height difference of a certain grid point before and after the opening operation is smaller than the height difference threshold set by the current iteration, it is recognized as a ground point, otherwise it is an object point.

3. IMPROVED MORPHOLOGY FILTERING ALGORITHM

3.1 Improved Window Size

The opening operation is a crucial step in the filtering algorithm of mathematical morphology (Hui et al., 2016). In view of the traditional mathematical morphology filtering algorithm, because of the small window size, the height difference between the two iterations is relatively small that resulting in some non-ground points being difficult to filter out and missing the ground point existing in the existing window size. In order to balance the algorithm execution efficiency and filtering performance, this paper continuously iterates the window size and the height difference threshold by improving the mathematical formula of the window size. According to the comparison filtering effect, the performance characteristics of the improved algorithm are analyzed.

For the determination of the window size of progressive mathematical morphology filtering, this is the core of the algorithm and one of the key points. There are some shortcomings in the method of determining the existing window size. In addition, since the size of the window is measured in millimeters, while the morphological operation is based on pixels. Therefore, the improved linear and exponential growth formulas of window size are given below for improvement and optimization:

$$\omega_k = [2(k+1) \times b + dh_0] \times cellsize \tag{7}$$

$$\omega_k = (2b^k + dh_0) \times cellsize \tag{8}$$

Where ω_k is the window size, k is the number of iterations, $k = 1,2,3,\cdots,M$, b is the initial window size, and dh_0 is the initial height difference threshold. A small height difference threshold and window increment speed are ensured while the window size changes.

3.2 Procedures for the Improving Method

Step 1： Grid virtual data and rasterize elevation data. The original LiDAR 3D point cloud data is gridded, and the minimum bound grid size is determined according to the maximum and minimum values in the x, y direction. Create a regular grid with the average spacing of the laser point, try to make each grid have at least one laser footpoint. The serial number of the laser point data is recorded in the corresponding grid, and a regular grid index is established for the laser point $(x,\ y,\ z)$:

$$\begin{cases} I = floor(x_i - x_{min})/cellsize \\ J = floor(y_i - y_{min})/cellsize \end{cases} \tag{9}$$

Where x_{min} and y_{min} are the minimum values of the xy plane range, and $cellsize$ is the grid size. Assign the lowest elevation value of all point cloud data in each grid to the grid unit. Due to the uneven distribution of point cloud data, some grid units don't exist laser point, and the nearest neighbor interpolation method is used for elevation interpolation, and the elevation value of the laser point closest to the grid unit is assigned to the grid unit. By establishing a virtual grid, the point cloud data is converted from a three-dimensional space to a two-dimensional space, which facilitates neighborhood search and subsequent filtering operations.

Step 2： Set parameters. Set the main relevant parameters: maximum window size, window size growth mode, slope coefficient s, initial height difference threshold dh_0, maximum height difference threshold dh_{max}. Set the window growth mode according to the terrain details and the distribution of features in the actual scene, and use the improved window size formula proposed above.

Step 3：Open operation .1) The progressive morphological filter whose major component is an opening operation is applied to the grid in window size $\omega_k \times \omega_k$. Enter the initial window size during the first iteration and calculate the height difference threshold of the current iteration. The output of this step includes a) the further smoothed surface from the morphological filter and b) the detected nonground points based on the elevation difference threshold. 2) The size of the improved filter window is increased and the elevation difference threshold is calculated. 1) to 2) are repeated until the size of the filter window is greater than a predefined maximum value. This value is usually set to be slightly larger than the maximum window size (This maximum is usually set to be slightly larger than the size of the largest building).

Step 4：Generate DEM based on the filtered data set.

4. EXPERIMENTAL VERIFICATION

4.1 Test Data

The LiDAR point cloud data is obtained from The third working committee of the International Society for Photogrammetry and Remote Sensing (ISPRS) (http://www.itc.nl/isprswgIII-3/filtertest/index.html). The data contains eight scenarios specifically designed to test filtering algorithms, including data for urban and rural areas, as shown in Table 1. The point cloud spacing in urban areas is between 1 and 1.5 m and between 2 and 3.5 m in rural areas. These data include plain, vegetation, buildings, roads, railways, bridges, power lines, waters and other topographical features, and 14 reference data representing different topographical features were extracted to test the filtering accuracy of the improved algorithm. The data given in Table 1 has been manually classified by the provider, and the LiDAR point cloud data are accurately classified into ground points and non-ground points. Researchers can perform qualitative and quantitative analysis of classification errors on the filtering algorithm (Zhang and Qi et al., 2016).

Sample	Features	Sample	Features
11	Vegetation and buildings on steep slopes	42	Elongated objects, Low and high frequency variation in the landscape
12	Small objects(cars)	51	Vegetation on slope
21	Narrow bridge	52	Low vegetation, Discontinuity-sharp ridge
22	Bridge (South west)/Gangway(North East)	53	Discontinuity preservation
23	Complex buildings, Large buildings, Disconnected terrain	54	Low resolution buildings
24	Ramp	61	Discontinuity-sharp ridge, ditches
31	Disconnected terrain, Low point, Low point influence	71	Bridge, Discontinuity-preservation

Table 1. Sample data for the testing algorithm

4.2 Precision Analysis

In order to reflect the filtering performance of the algorithm on the LiDAR point cloud data, the basic principle and algorithm flow of the progressive mathematical morphology filtering method based on the improved window size in Section 3 is presented. The main parameters of each test sample selected in combination with the actual scene topographical features are shown in Table 2.

Sample	Grid size / m^2	s	h_0 / m	h_{max} / m	Sample	Grid size / m^2	s	h_0 / m	h_{max} / m
11	2＊2	0.6	1	30	42	1＊1	0.1	0.4	5
12	2＊2	0.3	0.5	10	51	2＊2	0.5	0.2	30
21	1＊1	0.2	0.5	3	52	1＊1	0.5	1.2	50
22	1＊1	0.9	1	15	53	1＊1	1	1	40
23	1＊1	0.6	1	10	54	1＊1	0.2	0.2	50
24	1＊1	0.8	0.8	20	61	1＊1	0.6	1	50
31	1＊1	0.1	0.5	5	71	2＊2	0.5	0.6	10

Table 2. Filter parameters for each sample

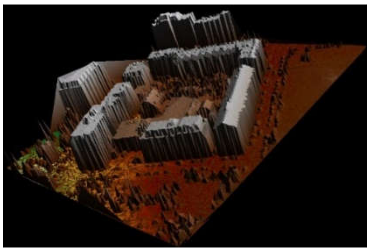

(a1) Before the filtering

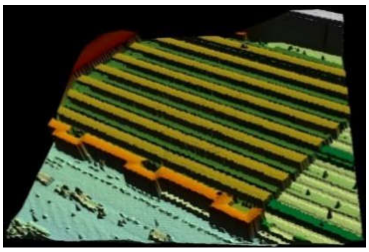

(b1) Before the filtering

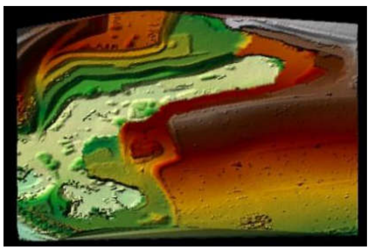

(c1) Before the filtering

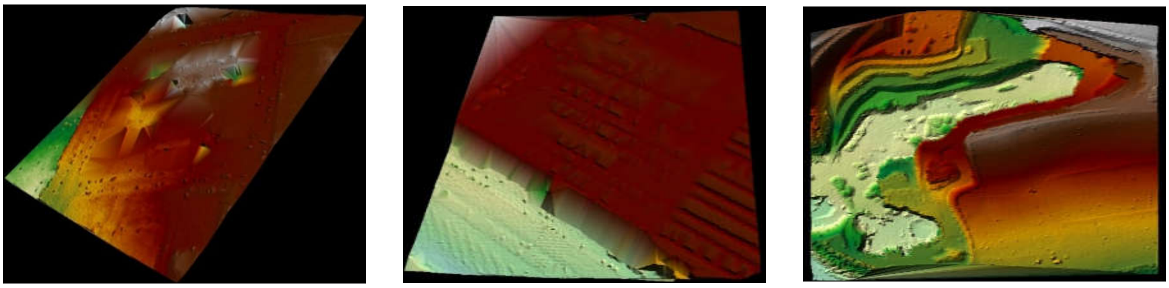

(a2) After the filtering (b2) After the filtering (c2) After the filtering

（a）Sample 31 (b) Sample 42 (c) Sample 53

Figure 2. The Original Point Cloud and Morphological Filter Results

Experimental results show that the improved method can effectively identify ground and non-ground points. As shown in Figure 2, the data of sample 31, sample 42 and sample 53 are used for analysis. The above three pictures are before the filtering, and the next three pictures are after the filtering. In Figure 2 (a), most of the ground details can be better preserved. At the same time, the building, some trees and vehicles in the adjacent building are effectively identified and filtered out. Figure 2 (b) demonstrates that the improved algorithm preserves the undulations of the terrain and better filtering at lower elevations. It can be observed in from Figure 2 (c) that in areas with complex terrain, the improved method not only preserves the detailed information of the ground, but also better filters out non-ground points on steep ridges and retains existing terrain features. In a word, proposed method in this paper solves the problem with excessive filtering and missing due to window size.

To more accurately analyze the results of this test, quantitative evaluation of the filtering effect is also crucial for the generation of high-quality DEM. The correct segmentation result is based on the manual classification results of each sample in the test area, and the classification error of the improved algorithm for each sample data is obtained. The definition of the classification error was given in table 3, including Type I, Type II and Total error. The total errors of proposed algorithm are compared with the eight traditional algorithm summarized in Reference (Sithole, Vosselman, 2003; Sithole, Vosselman, 2004), and given the average of the total error of the nine algorithm.

Category	Filtered		Total	Error / %
	Ground points	Object points		
Ground points	a	b	e=a+b	b/e (Type I)
Object points	c	d	f=c+d	c/f (Type II)
Total			n=e+f	(b+c)/n (Total)

Table 3. Definition of the filtering error

Among them a is the number of points in the filtering result where the ground points are classified correctly; b is the count of ground points rejected as objects; c the count of object points accepted as ground; and d is the number of points that are not correctly classified by the ground; e is the total number of ground points; f is the total number of object points.

Sample	Elmqvist / %	Sohn / %	Axelsson / %	Pfeifer / %	Brovelli / %	Roggero / %	Wack / %	Sithole / %	We / %	Mean / %
11	22.4	20.49	10.76	17.35	36.96	20.80	24.02	23.25	<u>10.31</u>	20.70
12	8.18	8.39	<u>3.25</u>	4.50	16.28	6.61	6.61	10.21	3.96	7.55
21	8.53	8.8	4.25	2.57	9.30	9.84	4.55	7.76	<u>2.02</u>	6.40
22	8.93	7.54	<u>3.63</u>	6.71	22.28	23.78	7.51	20.86	6.00	11.91

23	12.28	9.84	4.00	8.22	27.80	23.20	10.97	22.71	7.16	14.02
24	13.83	13.33	4.42	8.64	36.06	23.25	11.53	25.28	5.74	15.78
31	5.34	6.39	4.78	1.80	12.92	2.14	2.21	3.15	2.26	4.55
42	3.68	1.78	1.62	2.64	6.38	4.30	3.54	3.85	1.12	3.21
51	23.31	9.31	2.72	3.71	22.81	3.01	11.45	7.02	3.07	9.60
52	57.95	12.04	3.07	19.64	45.56	9.78	23.83	27.53	6.98	22.93
53	48.45	20.19	8.91	12.60	52.81	17.29	27.24	37.07	4.72	25.47
54	21.26	5.68	3.23	5.47	23.89	4.96	7.63	6.33	4.92	9.26
61	35.87	2.99	2.08	6.91	21.68	18.99	13.47	21.63	1.50	13.90
71	34.22	2.20	1.63	8.85	34.98	5.11	16.97	21.83	3.46	14.36
Mean / %	21.73	9.21	4.18	7.83	26.41	12.36	12.25	17.03	4.52	12.83

Table 4. Comparison of total errors for all samples of the nine representative filtering algorithms

It can be seen from the comparison in Table 4 that the total filtering error of each sample data is smaller than the average value, and the overall total error is second only to Axelsson. In the comparison of the total error minimum (underlined) of 15 sample data, the proposed method has high precision on complex terrain (such as sample11, sample53, sample61). At the same time, there is a higher accuracy in the terrain (such as sample21, sample42). The main features of sample11 and sample53 are vegetation and buildings on steep slopes. Most of the filtering algorithms have larger errors when testing the data. The total error of the algorithm in sample11 and sampl53 is 10.31% and 4.72%. The algorithm is 0.45% and 4.19% better than Axelsson's algorithm. The topographic structure of sample42 is obvious and regular. The proposed method can obtain better accuracy, which is 2.09% lower than the average total error. In summary, the algorithm of this paper fully verifies the superiority of the above sample data filtering compared with other traditional algorithms.

5 CONCLUSION

In the traditional mathematical morphological filtering algorithm, there are often some problems such as over-filtering of ground points and omission of non-ground points. Therefore, based on the principle of mathematical morphology filtering algorithm, an improved progressive mathematical morphology filtering method is proposed in this paper. By improved the mathematical formula of the window size in the mathematical morphology filtering algorithm, the window size and the corresponding elevation difference threshold are continuously iterated, which can effectively solve the problem of insufficient non-ground point filtering in LiDAR point cloud data filtering. The method is verified using the sample data which ISPRS provide for testing. The experimental results show that the proposed algorithm is robust in most complex scenarios, effectively removing target points while maintaining ground points to a large extent. All the types of error are controlled simultaneously in a relatively small interval and the better filtering performance for most regions are verified. Compared with the traditional filtering algorithm, the proposed method has higher accuracy in different terrains and the average total error is reduced by 8.31%. It shows that the proposed algorithm is versatile and reliable for LiDAR point cloud.

ACKNOWLEDGMENTS

This work was supported by National Natural Science Foundation (41461089).

REFERENCES

Axelsson, P., 2000. DEM generation from laser scanner data using adaptive TIN models. International Archives of the Photogrammetry. *Remote Sensing and Spatial Information Sciences*, 33 (Part 4B), 111-118.

Haralick, R.M., Sternberg, S.R., Zhuang, X., 1987. Image Analysis Using Mathematical Morphology, *IEEE Trans. Pattern Anal. Machine Intell.* vol. PAMI-9, 523–550.

Hui, Z.; Hu, Y.; Yevenyo, Y.Z.; Yu, X. An Improved Morphological Algorithm for Filtering Airborne LiDAR Point Cloud Based on Multi-Level Kriging Interpolation. *Remote Sens*. 2016, *8(1):* 35.

Kilian, J., Haala, N., 1996. Capture and evaluation of airborne laser scanner data. *Int. Arch. Photogramm. Remote Sens*, 31, 383-388.

Kraus, K., Pfeifer, N., 1998. Determination of terrain models in wooded areas with airborne laser scanner data. *ISPRS Journal of Photogrammetry and Remote Sensing*, 53(4), 193–203.

Li, Y., Wu, H., Xu, H., An, R., Xu, J., & He, Q. 2013. A gradient-constrained morphological filtering algorithm for airborne LiDAR. *Optics & Laser Technology*, 54, 288–296.

Luo, Y., Jiang, T., Gong Z., et al., 2009. An adaptive and multi-scale mathematic morphological filter for point cloud data filtering. J. *Geomatics Science and Technology*, 26(6), 426-429.

Mongus, D., & Žalik, B. 2012. Parameter-free ground filtering of LiDAR data for automatic DTM generation. *ISPRS Journal of Photogrammetry and Remote Sensing*, 67, 1–12.

Sithole, G., Vosselman, G., 2003. ISPRS Comparison of Filter [R/OL]. http://www.itc.nl/isprswgIII-3/filtertest/Report050802003.pdf.

Sithole, G., Vosselman, G., 2004. Experimental comparison of filter algorithms for bare-earth extraction from airborne laser scanning point clouds. *J. Photogrammetry & Remote Sensing*, 59(1-2), 85~101.

Sun, M., Gu, H., 2016. A New Filtering Method for Airborne LiDAR Data Based on Differential Morphological Profiles. *Journal of Geodesy and Geodynamics*, 36(7), 591-599.

Vosselman, G., 2000. Slope based filtering of laser altimetry data. International Archives of the Photogrammetry. *Remote Sensing and Spatial Information Sciences*, 33 (Part 3B), 935-942.

Wan, P., Zhang, W., Skidmore, A. K., Qi, J., Jin, X., Yan, G., Wang, T., 2018. A simple terrain relief index for tuning slope-related parameters of LiDAR ground filtering algorithms. *ISPRS Journal of Photogrammetry and Remote Sensing*, 143, 181–190.

Zhang, K., Chen, S.C., Whitman, D., Shyu, M.L., Yan, J., Zhang, C., 2003. A progressive morphological filter for removing nonground measurements from airborne LIDAR data. IEEE Transactions on Geoscience and *Remote Sensing*, 41 (4), 872-882.

Zhang, W., Qi, J.; Wan, P., Wang, H., Xie, D., Wang, X., Yan, G., 2016. An Easy-to-Use Airborne LiDAR Data Filtering Method Based on Cloth Simulation. *Remote Sens*, *8*, 501.